NASA

Technical Memorandum 85049

INTERPRETATION OF ^{3}He VARIATIONS IN THE SOLAR WIND

M. A. Coplan
K. W. Ogilvie
J. Geiss
P. Bochsler

JUNE 1983

National Aeronautics and
Space Administration

Goddard Space Flight Center
Greenbelt, Maryland 20771

INTERPRETATION OF ^{3}HE ABUNDANCE VARIATIONS IN THE SOLAR WIND

by
M. A. Coplan
Institute for Physical Science and Technology
University of Maryland

K. W. Ogilvie
Goddard Space Flight Center
Greenbelt, Maryland

P. Bochsler
J. Geiss
Physikalisches Institut
University of Bern

ABSTRACT

The ion composition instrument (ICI) on ISEE-3 has observed the isotopes of helium of mass 3 and 4 in the solar wind almost continuously between August 1978 and July 1982. This period included the increase towards the maximum of solar activity cycle 21, the maximum period, and the beginning of the descent towards solar minimum. Observations were made when the solar wind speed was between 300 and 620 km s^{-1}. For part of the period evidence for regular interplanetary magnetic sector structure was clear and a number of ^3He flares occurred during this time.

The long-term average $^4He^{++}/^3He^{++}$ flux ratio $\langle R \rangle$, was 2050 ± 200, in agreement with a previously reported result obtained using part of this data set, and in very good agreement with the previous measurements made over much shorter periods of time with the foil technique. The $\langle R \rangle$ values for 6-month intervals show statistically significant differences. The highest of these values is 2300 and coincides with the solar maximum of cycle 21 indicating that at solar maximum there may be changes in the character and rate of occurrence of short-term variations in $\langle R \rangle$. We also find that $\langle R \rangle$ drops under conditions of low proton flux in the solar wind, and that it is high when solar wind speeds are lowest.

At solar wind speeds above ~400 km s^{-1} $\langle R \rangle$ is nearly constant at about 2000; at lower speeds it is larger and more variable, in agreement with the idea that the sources of high and low speed wind are different. At times of sector boundary current sheet crossings, identified with coronal streamers, there is a characteristic rise in the value of $\langle R \rangle$ indicating an encounter with a plasma with reduced $^3He^{++}$ abundance. Autocorrelations have been computed for $^4He^{++}$, $^3He^{++}$ and $^4He^{++}/^3He^{++}$ and may indicate a correlation time of about 14, 20 and 20 hours respectively. Periods of duration of

about one day when R is less than 1000 tend to coincide with the observation of compound streams.

The possibility of detectable increases in $^3He^{++}$ flux in plasma which left the sun at the time of ^3He flares has been investigated, but no significant increase was seen.

INTRODUCTION

Since the first observations (Neugebauer and Snyder, 1966), the abundance of helium in the solar wind has been known to be highly variable, but the reasons for this variability have not been firmly established. Almost all systematic observations were of $^4He^{++}$, however the ion composition instrument (ICI) on the ISEE-3 spacecraft has now made continuous observations of both $^4He^{++}$ and $^3He^{++}$ for a wide range of solar wind conditions. In this paper we discuss these observations, with a view towards learning more about the phenomena which govern the abundance of ions in the solar wind.

In the 1960's, it became possible to identify a noble gas component in meteorites as being due to implantation at low energy. It was correctly argued that this component is made up of trapped solar wind particles, and isotopic ratios for noble gases in the solar wind including helium were deduced (Zähringer, Hintenberger et al., 1965; Eberhardt et al., 1965a, 1965b; Wänke, 1965), which are remarkably close to the ratios that were later directly determined.

Bame et al., (1968) were the first to detect $^3He^{++}$ directly in the present-day solar wind flow and found that rather large variations in the $^4He^{++}/^3He^{++}$ ratio do occur. A set of precise $^4He^{++}/^3He^{++}$ ratios in the solar wind were determined by the foil collection method during five Apollo lunar landings (1969-1972) covering periods ranging from one hour to two days (Geiss et al., 1972).

A solar wind $^4He^{++}/^3He^{++}$ ratio has also been obtained from laboratory analyses of the noble gases in a piece of the Surveyor spacecraft that was brought back to earth by the Apollo 12 crew (Bühler, et al., 1971; Warasila et al., 1974). The results obtained--representing irradiation by the solar wind over several years--were somewhat higher than the results from the foil

collection experiments. However, the He/Ne ratio in the Surveyor material indicates that a portion of the helium may have been lost by diffusion, introducing a source of error for the $^4He/^3He$ ratio deduced from that material.

Both the long term average abundance of ^3He and its short period variations, due for example to interplanetary and solar events, are of interest for at least three reasons:

1. A comparison between present-day foil collection data and studies of solar wind noble gases in young and old lunar material indicates that the abundance of $^3He^{++}$ in the solar wind has increased in the last 4.5×10^9y (Eberhardt et al., 1971; Geiss, 1973). However, the average ratio $\langle R \rangle = (^4He^{++}\text{flux})/(^3He^{++}\text{ flux})$ has dropped at most by 15% during the last 3 to 4×10^9y, and this provides a quantitative check on theories of solar mixing (Schatzman and Maeder, 1981; Geiss and Bochsler, 1982). Since only a limited number of exposures was used for determinations by the foil collection experiments, a value of $\langle R \rangle$ obtained over a longer period is desirable in order to obtain a representative long term average for the present-day solar wind, and check for consistency with the Apollo foil results.

2. Assuming that the relative abundance $^4He^{++}/H^+$ in the outer convection zone of the sun is the same as that in interstellar material, that is 0.08 ± 0.01 (Audouze, 1981) and taking the canonical value of $^4He^{++}$ in the solar wind to be 0.045 ± 0.005, the value given for the fast solar wind by Bame et al., (1977), we see that $^4He^{++}$ is definitely depleted in the rather steady flow out of coronal holes. It has been argued (Geiss, 1982) that this depletion of $^4He^{++}$ by a factor of about two in the solar wind from coronal holes occurs near the solar surface by a charge-neutral separation

processes, and that this is a result of the high ionization potential of helium.

The $^4He^{++}/^3He^{++}$ ratio in a solar prominence has been determined by Hall (1975). The value obtained was $2500 \begin{smallmatrix} + 2500 \\ - 830 \end{smallmatrix}$ to be compared to 2350 ± 120 as measured in the solar wind by the Apollo foil experiments (Geiss et al., 1972). Even if we assume that the isotopic ratio in the prominence was representative for the outer convective zone, we note that the error on the first figure is so large that it is not possible to determine by direct comparison whether $^4He^{++}$ is systematically depleted relative to $^3He^{++}$ in the solar wind. Since the ionization potentials of ^3He and ^4He are virtually identical, such depletions would be entirely due to the difference in mass of the two isotopes.

3. $^3He^{++}$, present in concentrations of a few parts in 10^5, is a true test particle in the solar wind, unlike $^4He^{++}$, which carries too high a proportion of the total momentum flux to fulfill this role. At the same time, $^3He^{++}$ is easily and cleanly isolated by the ICI mass spectrometer because it is the only species in the solar wind with a M/Q value between one and two. The $^3He^{++}$ ion is thus particularly well suited for use as a diagnostic particle.

The present investigation has been carried out both to arrive at a value of $^4He^{++}/^3He^{++} = \langle R \rangle$, averaged over a period of four years, and to study variations of $\langle R \rangle$ over periods between hours and months. The ISEE-3 orbit about the Lagrangian point between the sun and earth combined with the properties of the ICI ensure that $^3He^{++}$ can be measured almost continuously under most conditions in the solar wind; the most important exception is for flows with speeds in excess of 620 km s^{-1}. In a previous publication (Ogilvie et al., 1980a) we presented preliminary results based upon

observations made between August and November, 1978 and March and August, 1979. The overall abundance ratio, $\langle R \rangle$ was $2.1 \pm 0.2 \times 10^{3}$ for that period, in agreement with the measurements made using the foil collection technique (Geiss, et al., 1972). This paper reports both results of observations for extended periods, and observations of the behavior of the two helium ions associated with interesting changes occurring on the sun and in the interplanetary medium. These provide evidence for the importance of coulomb interactions and for the occurrence of fractionation processes in the solar corona.

INSTRUMENTATION

The design, construction, and calibration of the ICI have been described by Coplan et al., (1978) and its modes of operation have been described in several publications of the group (Ogilvie et al., 1980a, 1980b; Kunz et al., 1983). Here we merely state that a M/Q spectrum over the range from 1.4 to 6.0 is observed with a resolution (M/ΔM) if 20 to 30 every 30 minutes, during periods when the solar wind speed falls between 300 and 620 km s^{-1}, which is ≈90% of the time during the period studied here. The spectra are typically recorded at seven velocity intervals centered about the solar wind velocity. The resolution is sufficient to measure $^{3}He^{++}$ (M/Q = 1.5) in the presence of the much larger fluxes of protons and $^{4}He^{++}$ (M/Q = 2). Correction for the instrumental background is discussed in the next section.

Since this investigation covers a period of four years, a remark about long term stability is required. The detectors are channel electron multipliers (CEM), and they had recorded less than 10^{10} counts by the end of the period covered. The present background counting rate, 0.2 s^{-1}, does not

differ appreciably from the background measured in the solar wind soon after launch. The construction of the detector housing incorporates two grids in front of the detectors; the first one is grounded and the second one is maintained at the potential of the CEM input to ensure that all secondary electrons are collected. Periodic checks were performed to monitor the counting efficiency by changing the CEM voltage and observing the counting rate. These checks indicate that the properties of the detectors have not changed, and since most of the results concern the ratio $^4He^{++}/^3He^{++}$, it is unlikely that long term changes in the instrument have influenced any of the variations discussed here.

DATA REDUCTION

In the normal mode of operations, M/Q-velocity scans are routinely obtained twice per hour. After correction for instrumental background and detector dead time are made, the solar wind (helium) speed is calculated from parabolic fits to the data from the $^4He^{++}$ searches and scans, after weighting the counts with the inverse fourth power of the corresponding velocity to convert them to quantity proportional to the distribution function. The $^4He^{++}$ temperature and density are then calculated by fitting to the data a maxwellian velocity distribution function convected at this speed and convoluted with the measured instrument function. Because of the low flux of $^3He^{++}$ ions, their bulk speed is not determined separately but is taken equal to that of $^4He^{++}$; the $^3He^{++}$ temperature is assumed to be 3/4 of the $^4He^{++}$ temperature. These assumptions have been tested for these two ions and are generally satisfied (Ogilvie et al., 1980b). Various tests are incorporated in the reduction program to eliminate data of questionable validity, with the result that the uncertainty in an individual flux ratio

R mainly results from the statistical uncertainty of the $^3He^{++}$ flux, typically ≈25%. The $^4He^{++}$ flux determination has a statistical uncertainty of a few percent. Because both helium isotopes are taken to have the same speed, flux and density ratios are the same. The average quantity <R>, which is the sum of $^4He^{++}$ fluxes divided by the sum of $^3H^{++}$ fluxes, is directly comparable to the result of the foil collection method, in which helium atoms implanted in the foil are later released by heating and analysed by laboratory mass spectrometry.

Figure 1 shows how the relative sensitivity of the instrument to $^3He^{++}$ and $^4He^{++}$ ions varies with solar wind speed; note that the sensitivity is uniformly grater for $^3He^{++}$ than for $^4He^{++}$, and the ratio varies smoothly between 1.6 and 2.8 with solar wind speed.

As an example of the observations, Figure 2 shows a plot of the measured $^3He^{++}$ flux, $^4He^{++}$ flux, and abundance ratio covering the period from August 18 to December 27, 1978. Hourly average values are plotted, and the data gaps crossed by straight line segments. This period was typical in that an almost complete time series of observations was obtained. Superposed on the point-to-point $^3He^{++}$ fluctuations, are slower variations which are seen to correlate well with those of the $^4He^{++}$ flux, whose statistical fluctuations are too small to be seen in Figure 2. It is clear that many of the variations shown in the lower trace in Figure 2 are statistically significant, and represent real physical changes in the isotopic constitution of the solar wind. However, because the dynamic range available for $^3He^{++}$ measurement is smaller than that for $^4He^{++}$ measurement, ratio changes caused by reductions in the $^3He^{++}$ flux must be carefully examined. On the right-hand side of the top trace in Figure 2 there is a scale of counts, giving an approximate measure of the number of counts which go into the $^3He^{++}$ flux

determination; $^3He^{++}$ flux levels below 10^7 $m^{-2}s^{-1}$ are characterized by signal/noise ratios less than unity, fluxes above that level are relatively accurately determined.

The uncertainty in R has both instrumental and statistical contributions. Among the instrumental contributions are calibration uncertainties, detector noise, and detector dead time. The calibration uncertainties are those associated with the determination of the sensitivity ratios plotted in Figure 1. From an analysis of the calibration procedure we estimate that the curve in Figure 1 is accurate to 10% or better over the full range of solar wind velocities. Detector noise is of the order of 0.2 count/second and has remained constant throughtout the life of the experiment. Detector dead time corrections are routinely applied and are only significant for the highest $^4He^{++}$ fluxes which generally occur at low solar wind speeds.

Since the background count rate is not negligible compared to the $^3He^{++}$ count rate, the value of R depends directly upon an accurate knowledge of the background. For the present determinations, a separate background was obtained for each M/Q-velocity spectrum by averaging the counts in the M/Q channels (M/Q = 1.45 and M/Q = 1.56) adjacent to that for $^3He^{++}$ (M/Q = 1.5).

As an example take a typical case with 15 net $^3He^{++}$ counts and a total background of 3 counts. The statistical uncertainty is $\sqrt{18 + 3} = 4.6$. Under some circumstances the statistical uncertainty is considerably larger and we have rejected all data where the ratio of net $^3He^{++}$ counts to net background counts is less than 0.5, in addition to rejecting all data where the background exceeds five times the normal detector background. Periods having high background usually coincide with solar particle events, during which high energy particles can penetrate the spacecraft and stimulate the detectors directly.

TABLE I

Periods	Number of Observation	<R>	R_{MP}	Correlation Coefficient	Sun Spot Number
78b	1871	1970	1200	.74	104
79a	2529	1920	1200	.70	126
79b	1921	1950	1580	.75	153
80a	603	2300	1500	.68	160
80b	1461	2080	1500	.73	148
81a	2545	2050	1500	.69	140
81b	1951	2230	1500	.73	140
82a	1627	2100	1400	.65	128
TOTAL	14508	2050±200	1500	.72	

LONG PERIOD CHANGES IN $^3He^{++}$ ABUNDANCE

In this section of the paper we describe our observations of $^3He^{++}$ abundance averaged over the whole four year period, which includes the maximum of solar cycle 21 in 1980. For covenience we have divided this period into eight intervals ranging in length from 100 to 184 days. The gaps in the data were due either to spacecraft tracking problems, solar proton events, or operation of the instrument in a mode in which observations of $^3He^{++}$ were not made.

Since large values of R can correspond to small $^3He^{++}$ fluxes, the background correction is especially important. Although we have excluded large solar proton events from the data the presence of small events could increase the uncertainty in R for those periods. However, the method used to determine the background, together with our policy of rejecting observations with signal/noise ratio less than .0.5, reduces the effect of such small events on the total data set.

Figure 3a shows a histogram of the distribution of values of R derived from the whole data set. The average value, $\langle R \rangle = 2050 \pm 200$, agrees extremely well both with the value of 2100 ± 200 obtained from the shorter data set (Ogilvie, 1980a) and with the results of previous determinations of ^3He abundance in the solar wind, using the foil collection technique $\langle R \rangle = 2350 \pm 120$ (Geiss et al., 1972). If the histogram of the total set is redrawn as a weighted distribution, using the $^3He^{++}$ count as weight for each individual observation, the most probable and average values remain the same, well within the error given, while the "tail" towards high values of R is reduced.

Figure 3b shows a histrogram of $1/R$ $(^3He^{++}/^4He^{++})$, included to emphasize the distribution of small values of R.

In Table I the observations of R are divided into eight roughly equal periods of six months duration. These cover the four year interval from August, 1978 through June, 1982, and their relationship to the solar activity cycle is shown by the smoothed sun spots numbers in Table I. We see that during the four years the sun spot number rose from ~100 to a maximum of 160 in period 1980a, and then decreased to ~130 again. The value of $\langle R \rangle$ deduced from the 14,508 observations with signal-to-noise greater than 0.5 and background less than five times normal, is 2050 ± 200. The rejection criteria were chosen as a way of eliminating data of questionable validity; however, since they also selectively eliminate low $^3He^{++}$ fluxes, they may have the effect of introducing a bias into our sample. The criteria are thus a compromise between the inclusion of unreliable data on the one hand and the introduction of bias into the data set on the other. The largest value of $\langle R \rangle$ over a six month interval is 2300, slightly more than one standard deviation above the overall value. This was measured during the period when solar activity was at its maximum. The variation between the two periods near solar maximum, when the sun spot number was ~150-160, and the earlier and later periods when the sun spot number was 110-120 gives a measure of the variability of $\langle R \rangle$ with solar activity. Although the effect is small, some events associated with solar activity, and therefore more common near solar maximum, apparently cause increases in the isotopic ratio $^4He^{++}/^3He^{++}$ in the solar wind. Comparison of the present data with monthly averages of A_p (Sugiura, private communication, 1983) indicates no significant coincident variations in the two quantities.

Figure 4 is a contour map of the correlation between the logarithms of the fluxes of $^3He^{++}$ and $^4He^{++}$. Because the uncertainties are mostly due to the $^3He^{++}$ statistical fluctuations, the observations are weighted by the

number of $^3He^{++}$ counts as explained above. The contour lines connect points of equal density of weighted observations, and the increments between lines are given in the figure. The contours are pear shaped; at the higher fluxes the data lie in a narrow band about a diagonal; at lower fluxes the correlation is less strong. This may be intrinsic or the result of counting statistics. We have also plotted as single points the results obtained in the interplanetary medium by the five Apollo foil experiments (Geiss et al., 1972); clearly, there is good agreement between the results of these very different techniques. The effect of the measurement times, up to 45 hrs in the longest Apollo experiment, is to smooth the foil data, and that there is accordingly less variability among the five Apollo observations than for the ICI data set.

In order to assess the influence of statistical fluctuations we have investigated a simple statistical model with a constant ratio $R = 2300$, and a log-normal distribution of $^4He^{++}$ fluxes centered about a flux of $8 \times 10^{10} m^{-2} s^{-1}$, with a threshold of $5 \times 10^{+7}$ counts/m^2s for $^3He^{++}$.

We have convolved the flux distribution $P_1(\log(^4He^{++}\text{flux}))$ with $P_2(n|\log(^4He^{++}\text{ flux}))$, the conditional probability to obtain n $^3He^{++}$ counts at a given $\log(^4He^{++}$ flux). Since there is a definite relation between R, n and the $^4He^{++}$ flux, we obtain P_3 (log R) by a transformation of variable n to log r and evaluate the integral

$$P_3(\log R) = \int_{-\infty}^{\infty} P_1(\log(^4\text{He flux})) \cdot P_2(\log R|(\log(^4\text{He flux}))d(\log(^4\text{He flux})).$$

The distribution P_3 resembles a log-normal distribution with a tail towards high ratios, and a most probable value of 2300. The width of the distribution is 0.2, corresponding to a factor of 1.6 in R, and much smaller than the width of the observed distribution. This indicates that

counting statistics cannot account for the whole of the extreme values of R in the observed distribution. Additional uncertainties in the data procedure, such as errors in the individually determined background corrections, could add to the spreading, but not sufficiently to account for all of it. We therefore conclude again that there are values of R which are considerably different form $\langle R \rangle$ as a result of physical causes, and this evidence is supported by the time-coherence of such values.

Figure 6 shows the distribution of the whole data set of observations of R on normal probability paper. This type of plot emphasizes the extreme values of R (Gumbel, 1958). If the data were distributed normally they would lie on a straight line. It is clear that a normal distribution does not describe the observations well over the whole range of observed variability of R. A simple calculation shows that, with respect to counting statistics, the signal/noise ratio is less than 1 when $R \gtrsim 3500$. Thus, single values of $R > 5000$ are poorly determined, while lower values are relatively well known. Nonetheless, as already discussed, both high and low values usually represent "real" fluctuations--those which can be related to changes in the isotopic abundance of helium in the solar wind.

In Table I we show the computed values of $\langle R \rangle$ and the most probable value R_{MP} of R for each of the eight sub-intervals, and in Figure 7 we show histogram plots for each of them. The histograms are remarkably similar within expected statistical fluctuations, except for the period around solar maximum, referred to as 1980a in the data set. As suggested earlier, a likely cause for the differently shaped histogram for this period, with a value of $\langle R \rangle$ somewhat more than one standard deviation above the overall value of $\langle R \rangle$, is a small solar activity effect. Table I also shows values of the correlation coefficients between the $^3He^{++}$ and $^4He^{++}$ fluxes, calculated

for each period. There are significant differences among the correlations, yet the average value of 0.72 indicates considerable coherence between the fluxes on a time scale of approximately 1 hr. A higher coefficient of correlation would be expected in the absence of statistical fluctuations, which are quite large for $^3He^{++}$. It is certainly to be expected that the two isotopes of helium should behave in the same general way, but that their behavior should sometimes differ because of their different mass. It is probably not accidental that a locally lower correlation occurs at solar maximum, indicating that during periods of high solar activity there are more corona-associated changes, in contrast to changes near the solar surface or dynamical changes in the interplanetary medium, which would be expected to affect both species in about the same way.

Figure 7 shows plots of autocorrelations of the logarithms of the fluxes of $^4He^{++}$ and $^3He^{++}$ and of the $^3He^{++}/^4He^{++}$ ratio. These are derived from data smoothed over 3 hours. The correlation time is 14 hrs for $^4He^{++}$, and it is 20 hrs for $^3He^{++}$ and the isotopic ratio. It is remarkable that we obtain a larger correlation time for $^3He^{++}$ than for $^4He^{++}$, because the statistical fluctuations in the $^3He^{++}$ data should result in a shortening of the autocorrelation time. On the other hand, we cannot exclude that the selection criteria for $^3He^{++}$ could have lengthened its correlation time. Nevertheless, we like to point out that the difference between the autocorrelation curves of $^3He^{++}$ and $^4He^{++}$ could very well indicate that the $^4He^{++}$ flux shows stronger short-time variations than the flux of other ions.

VARIATION OF THE ISOTOPIC RATIO WITH FLUX AND VELOCITY

Figure 8a shows the $^4He^{++}$ flux in 25 km s^{-1} intervals, it is constant

to ±10 percent over the velocity range from 300 to 600 km s^{-1}. Since

$$\text{Flux}(^4He^{++}) = \text{Flux}(H^+) \times \text{Relative Abundance}(^4He^{++}),$$

and since the flux of hydrogen rises at low speeds, this implies that the abundance of helium is less at low than at high solar wind speeds, in agreement with the ideas of Hirshberg et al., (1972), and Borrini et al., (1983).

In Figure 8b we show values of $\langle R \rangle$ using the whole data set exhibited as a contour plot. Above ~375 km s^{-1} $\langle R \rangle$ is nearly constant at about 2000 below that speed there is an apparent rise to values of order 3000. We now discuss whether this rise could be due to an instrumental effect.

A possible cause of an apparent change in $\langle R \rangle$ at low speeds could be violation of the assumption $T(^3He^{++}) = 3/4\ T(^4He^{++})$, which is made in the course of data reduction. This assumption is based on the proportionality of kinetic temperature to mass, which often holds in the solar wind (Schmidt et al., 1980; Ogilvie et al., 1980a). However, coulomb collisions destroy this proportionality and result in a trend towards a single kinetic temperature for all species. Such collisions occur predominately at high densities, and thus low speeds. Since the mass ratio is small, one expects temperature effects to be small--calculations confirm this, and the effect cannot account for the observed change in $\langle R \rangle$ with velocity. A correction has been made to the data to remove the variation in instrument function with mass per charge and velocity. Although this correction is largest at low speeds, Figure 1 shows that it is small compared with the effect shown in Figure 8b and its onset is not so rapid. Thus the increase in $\langle R \rangle$ at low velocities is difficult to explain as purely instrumental.

Geiss et al., (1970) have considered the question of the acceleration of minor ions into the solar wind as a result of coulomb drag between them and

the protons in the low corona. They introduced the idea of a minimum proton flux required to incorporate an ionic species into the solar wind, and pointed out that the highest minimum flux for elements lighter than iron is required for the acceleration of $^4He^{++}$. $^3He^{++}$, however, requires a minimum flux only ~60% that of $^4He^{++}$, not appreciably different from that required for other ionic species. The model of Geiss et al., (1970), was extended by Borrini and Noci, (1979), to non-radial expansion. Hollweg, (1981), used an isothermal approximation and obtained very similar relations for the minimum fluxes of these ions. Clear evidence of a correlation between the abundance of any species and the proton flux has not been obtained. This was foreseen by Geiss et al., (1970), and is because the solar wind flux is a function of many parameters, and also because material observed at 1 AU could be a mixture from various flow tubes connected to various coronal positions, (Bochsler, 1982). Strictly speaking, the steady-state models investigated by Geiss et al., (1970), do not necessarily apply to the real solar wind, where different layers in the corona may not have reached the steady state equilibrium.

Because the isotopes of helium differ only in mass, many effects which would cause variations with solar wind flux of the abundance of a single ion do not affect the variation of the ratio R. Thus it is worthwhile to study the variation of $\langle R \rangle$ with the flux of protons in the solar wind, illustrated for the present data set in Figure 9. The proton flux was obtained from the ISEE-3 data pool tape and the histogram shows the number of observations in each flux interval. There is a tendency for high ratios to coincide with high fluxes, and low ratios with the lowest fluxes, although there are few observations in the lowest category. This indication that low values of $\langle R \rangle$ coincide with low proton fluxes provides substantial evidence for the importance of coulomb collisions in the acceleration process, and is

consistent with the suggestion of Geiss et al., (1970), that $^4He^{++}$ requires significantly higher fluxes to accelerate into the solar wind than $^3He^{++}$.

DAILY AND HOURLY VARIATIONS

The variability of the relative density of $^4He^{++}$ ions in the solar wind has never been adequately explained (Neugebauer, 1981) although it most probably has its origin in the acceleration processes. Variations over periods of hours and days are pronounced in the $^3He^{++}$ and in the $^4He^{++}$ flux. For example, Grünwaldt, (1976), describing observations made by the plasma instrument of the HEOS 2 spacecraft, reported a 48 hr. period of particularly low solar wind speed (<300 km/s) during which the value of R remained at about 540 as a result of the reduction in the $^4He^{++}$ flux. The histograms in Figures 3 and 6 show that such a value of R is not exceptional, and we have shown that the flux $^3He^{++}$ varies more at low than at high speeds; however 48 hours is a long period of time for such a deviation from the most probable value to persist.

In studying variations on a daily or hourly time scale with the present data set, for which the $^4He^{++}$ flux is much better determined than the $^3He^{++}$ flux, we will not attempt to interpret gross correlations, but will measure variations of the $^3He^{++}$ flux at times close to the occurrence of known variations of the $^4He^{++}$ flux.

One well documented variation of this class is that observed when the spacecraft passes through the solar equatorial current sheet at a sector boundary. The current sheet is identified by Howard and Koomen, (1974) and Gosling et al., (1981) with the crossing of a coronal streamer, within which there is dense, slowly flowing plasma having a low helium abundance, n_α/n_p, observed at the same time as the magnetic field reversal.

Borrini et al., (1981) have made a superposed epoch analysis of proton density, velocity and temperature, and helium abundance, temperature ratio and velocity difference at 74 well defined sector boundaries from the Los Alamos Imp 6, 7 and 8 data set. They found that the helium abundance ($^4He^{++}$ predominately) dropped sharply at the time of the boundary crossing. The temperature ratio also showed a drop from ~5 to ~3. They interpreted their result as a coronal signal, providing evidence for gravitational fractionation in the corona, in agreement with the interpretation of helium enhancements in the driver gas of flare associated interplanetary shocks. Such enhancements are generally believed to characterize $^4He^{++}$-rich material from the lower corona expelled into the interplanetary medium as a result of the flare process (Hirshberg, 1970). Borrini et al., (1981) hypothesized that the abundance of helium decreases with height in the solar corona, and becomes fixed at a greater height in a streamer than elsewhere. If this is true one might expect that the ratio $R = [n(^4He^{++})/n(H^+)]/[n[^3He^{++})/n(h^+)]$ would show a change as the boundary is crossed, since at that point the streamer is being sampled.

We have investigated this matter using observations taken at the times of 17 clear sector boundary crossings in 1978, 1979, and 1981, taking zero epoch as the time of boundary crossing as given by the magnetometer (Interplanetary medium data book, supplement 2, 1983). In order to reduce statistical errors, we have included both stream-associated and stream-free events in our data set. The results are shown in Figure 10, where we plot the $^4He^{++}$ flux, and $^3He^{++}$ flux and the ratio R for ±3 days about the zero of time. Borrini et al. show, in their Figure 7, that the proton density increases by approx. 3.5 times around zero time, while n_α/n_p decreases from 4.5 to 3 percent. Thus the helium density increases by about 2.3 times,

and the flux by about 2 times over its value prior to the sector boundary crossing, in agreement with the plot in Figure 11. At the zero of time both $^4He^{++}$ and $^3He^{++}$ fluxes increase, the latter by a smaller amount so that R increases to ~4000. Note also the similar increase of R in the low speed region preceding the boundary crossing. Although of limited accuracy, the observations discussed here are in agreement with the overall rise in $\langle R \rangle$ at speeds below 360 km s^{-1} shown in Figure 9.

We now consider occurrences of periods of abnormally low values of R, defined for our purposes as sustained observations of $R < 1000$. We have searched the data set, in the form of plots of solar wind speed, $^4He^{++}$ density, R, and $^4He^{++}$ temperature, and find that in 15 out of at least 19 cases, such decreases of R were associated with streams having two velocity maxima, probably compound streams (Ogilvie and Burlaga, 1974). Figure 12 shows four examples of the effect; at the time of the second velocity maximum, there is a drop in $^4He^{++}$ density, so that the drop in R results from a smaller decrease in $^3He^{++}$ than in $^4He^{++}$. We have been unable to explain this effect as instrumental. A more quantitative study will be required to understand the causes of these variations, but meanwhile we point out that the interaction of two high speed flow systems may be involved, and that the variation might therefore be produced in the corona.

We now consider the question of whether the $^3He^{++}$ abundance in the solar wind is affected by the occurrence of so called ^3He flares. These are small solar flares, which cause the observed flux of $^3He^{++}$ in the MeV/nucleon energy range to be increased by as much as 10^3 (Hsieh and Simpson, 1970, Garrard, et al., 1973; Reames and von Rosenvinge, 1981). There are sometimes coincident increases in the Fe/He ratio at MeV/nucleon energies. Theories of this effect have invoked both nuclear reactions and

heating of $^3He^{++}$ by waves, excited by an instability in the coronal plasma, which resonate with the cyclotron frequency of $^3He^{++}$, (Fisk, 1978). If either of these processes change the composition of material in the solar wind acceleration region, a change of $^3He^{++}$ flux might be detectable at 1 AU at an appropriate time after the flare. Using a list of ^3He flares observed in the energy range 1.3 to 1.7 MeV/nucleon, kindly supplied by D. Reames (private communication, 1982) seven events were selected for which there was no coincident solar proton enhancement. Taking t_{i1} and t_{i2} as the beginning and end of the i^{th} event we calculated the ratios

$$\langle R(T)\rangle = \sum_i \sum_{t_{i1}-T}^{t_{i2}-T} {}^4He^{++} \Big/ \sum_i \sum_{t_{i1}-T}^{t_{i2}-T} {}^3He^{++}$$

where T is a lag time with the values -4, -3, -2, ... +3, +4 days. T = 0 corresponds to the beginning of the flares plus 3 days, the transit time of the solar wind. If the process responsible for the enhancement of ^3He at MeV energies also, for example, enhanced $^3He^{++}$ in the solar wind, we would expect a decrease in $\langle R\rangle$ at T = 0. Figure 13 shows the results; although there is a small decrease in $\langle R\rangle$ at about the expected lag time it is less than the standard deviation of the observations.

CONCLUSIONS

We have shown that the long term average $^4He^{++}/^3He^{++}$ ratio is in good agreement with the average derived from the five foil collection experiments, and that there is a small variation with solar activity which appears to be significant. Both increases and decreases of R, resulting from events on the sun and in the interplanetary medium, do occur, and their frequency of occurrence appears greater near solar maximum than near solar minimum.

Overall, the fluctuations in the isotopic fluxes are only moderately well correlated (0.72). Part of the lack of perfect correlation is due to counting statistics with the remainder associated with real physical fluctuation. Because of this and the properties of the distributions, we conclude that statistical fluctuations due to the low $^3He^{++}$ counting rate are not primarily responsible for the long tails above in the histograms shown in Figure 3, but that there are real though poorly determined fluctuations. Investigating the variation of R with solar wind speed indicates that R remains more nearly constant above than below ~400 km s^{-1}, Bame et al., (1977) showed that the high speed solar wind is different from the low speed wind, whose source regions are less certain, and in some respects more fundamental. According to this picture (Hansen and Koomen, (1974), Borrini et al., (1983), the source of most of the low speed wind is coronal streamers. Figure 9 therefore confirms that the abundance of helium is lower at low speeds than at high speeds, and indicates that the abundance of $^3He^{++}$ drops more than that of helium $^4He^{++}$ at these times. Not all the high speed solar wind observed here was associated with coronal holes, however, as the present data was taken in relatively disturbed conditions around solar maximum, while the observations of Bame et al, (1977) were taken during the years of decreasing solar activity, 1971-1974. Taking our value of $\langle R \rangle$ at high speeds flows (1900 ± 200] and the Bame et al. value for n_α/n_p, of 0.045 ± .005 we obtain a $^3He^{++}$ relative abundance of $2.4 \pm 0.2 \times 10^{-5}$ in these flows.

Autocorrelations were computed for the logarithms of both the $^3He^{++}$ and $^4He^{++}$ fluxes, and the results show that the correlation times are consistent with the expected dimensions of sources of particular "parcels" of solar wind which rotate with the sun past the subspacecraft point.

We have also found that there are periods of low R, at the time of coumpound streams, which are associated with drops in $^4He^{++}$ flux. Because of the correlation with streams, the low R values could be due to interactions in the interplanetary medium and not from changes at the source.

Turning to shorter period variations, we have investigated the changes in $^3He^{++}$ at magnetic sector boundary crossings. Using the results of Borrini et al., (1981) and making a superposed epoch analysis, we find an increase in $\langle R \rangle$ with a maximum just before the boundary crossing. At the sector boundary crossing the rise in $^4He^{++}$ flux is greater than that of the $^3He^{++}$ flux. The increase of R occurs throughout the period of low speed adjacent to the crossing.

Figure 10 shows the variation of $\langle R \rangle$ with proton flux for the subset of data for which proton parameters are available from the ISEE-3 data pool tape. Direct investigations of a correlation between proton flux and the abundance of $^4He^{++}$ in the solar wind have been unsuccessful because of the many interfering phenomena which affect the measurements. However, the abundance ratios are less subject to difficulties of this nature and the result shown in Figure 10 provides indirect evidence that coulomb collisions with protons are important in the acceleration of $^4He^{++}$, and presumably other ions, to form the solar wind. This does not explain the general increase of $\langle R \rangle$ at low speeds, Figure 9, since although high proton fluxes occur at the lowest speeds, the $^4He^{++}$ flux does not increase at low speeds; $\langle R \rangle$ changes because the $^3He^{++}$ flux drops.

The sector boundary observations also show that the increase in the proton flux is accompanied by an increase in $^4He^{++}$ flux; there is less change in the $^3He^{++}$ flux. We suggest that the $^4He^{++}$ flux is controlled by the acceleration mechanism, which draws flux from a reservoir, possibly

provided by gravitational fractionation. The $^3He^{++}$ flux is controlled by the characteristics of the source, which is different for low speed and high speed solar wind. At low speeds $\langle R \rangle$ rises (Figure 9), the $^4He^{++}$ flux changes little but the $^3He^{++}$ flux falls to a value similar to that observed at a sector boundary.

These results suggest that $^4He^{++}$ is definitely anomalous, both because it has a lower coulomb drag per unit mass, and because it is subject to mass fractionation. $^3He^{++}$, on the other hand, appears to be easily removed from the corona by common solar wind proton fluxes, but its supply to the slow solar wind may be restricted compared to the supply to the fast wind. Following ideas of Pneuman and Kopp, (1970), Borrini et al., (1983) have suggested that all slow solar wind comes from coronal streamers. Since the values of $\langle R \rangle$, $^3He^{++}$ flux and $^4He^{++}$ flux are the same within the present uncertainties for streamers and for slow solar wind, this suggestion cannot be ruled out and should be investigated further.

ACKNOWLEDGEMENTS

The authors wish to acknowledge useful discussions with L. F. Burlaga, E. W. Montrol, M. Schlesinger, and M. Dozzi. Partial support through NASA grant NAS 5-25472, the Computer Science Center of the University of Maryland and the Swiss National Science Foundation is gratefully acknowledge.

FIGURE CAPTIONS

Figure 1 The ratio of the sensitivity of the ICI to $^3He^{++}$ and $^4He^{++}$ ions as a function of the ionic velocity; data from laboratory measurements.

Figure 2 $^3He^{++}$ flux, $^4He^{++}$ flux and $^4He^{++}/^3He^{++}$ flux ratios for the period August 18-December 27, 1978. The data are hourly averages with data gaps spanned by straight lines.

Figure 3a Histogram of the log of the flux ratios $^4He^{++}/^3He^{++}$ for the whole data set. The average value $\langle R \rangle = 2050 \pm 200$.

Figure 3b Histogram of the inverse flux ratio $^3He^{++}/^4He^{++}$ for the complete data set. This histogram emphasizes the data at high $^3He^{++}$ flux.

Figure 4 Contour map of log(flux($^4He^{++}$)) vs log(flux($^3He^{++}$)). The contour intervals are marked on the figure. Five Apollo observations are also plotted and adentified by the corresponding flight numbers (11-15).

Figure 5 Integral probability of observing a given value of R as a function of the reduced flux ratio, R^*. A straight line is indicative of a normal distribution. Data is shown for the whole data set, open circles, and for period 1980a, dota.

Figure 6 Histograms of the distributions of R values for the eight periods detailed in Table I.

Figure 7 Plots of auto-correlations of log flux($^4He^{++}$) log flux($^3He^{++}$) and log($^4He^{++}/^3He^{++}$) vs time lag. The quoted correlation times correspond to the times at which the autocorrelation coefficients decrease to 0.37 (1/e).

Figure 8a $^4He^{++}$ flux as a function of a solar wind speed for the full data set

Figure 8b Contours of $\langle R \rangle$ as a function of solar wind speed for the full data set.

Figure 9 $\langle R \rangle$ as a function of proton flux (from ISEE-3 data pool tape).

Figure 10 Superposed epoch analysis for 17 well marked sector boundaries. Top trace, R; middle trace, flux ($^3He^{++}$); lower trace, flux $^4He^{++}$. The zero of time is the time of the change in magnetic field azimuth. Both stream associated and stream-free events are included.

Figure 11 Some events during which the value of R decreased to below 1000. Note that all are associated with the leading edges of compound streams, and coincide with large drops in the density of $^4He^{++}$.

Figure 12 Superposed epoch analysis for seven ^4He flare events. Shown is the overall value of $\langle R \rangle$ as a function of time lag where zero time is the time of the flare plus the solar wind transit time (3 days).

REFERENCES

Audouze, J., paper presented at "Study Week on Cosmology and Fundamental Physics," Vatican 1981.

Bame, S. J., A. J. Hundhausen, J. R. Asbridge, and I. B. Strong, "Solar Wind Ion Composition," Phys. Rev. Lett. 20, 393, 1968.

Bame, S. J., J. R. Asbridge, W. C. Feldman, J. T. Gosling, "Evidence for a structure free state at high solar wind speeds," J. Geophys. Res., 82, 1487, 1977.

Borrini, G., J. T. Gosling, S. J. Bame, W. C. Feldman, J. M. Wilcox, "Solar wind helium and hydrogen structure near the heliospheric current sheet," J. Geophys. Res. 86, 4565, 1981.

Borrini, G. and G. Noci, "Dynamics and abundance of ions in coronal holes," Solar Phys., 64, 367, 1979.

Borrini, G., J. T. Gosling, S. J. Bame, W. C. Feldman, "Helium abundance variations in the solar wind," Solar Phys 83, 367, 1983.

Bühler, F., Eberhardt, P., J. Geiss, and J. Schwarzmuller, "Trapped solar wind helium and neon in Surveyor 3 material," Earth Planet. Sci. Lett. 10, 297-306, 1971.

Burlaga, L. F., "Interplanetary streams and their interaction with the earth," Space Sci. Rev. 17, 327-1975.

Coplan, M. A., K. W. Ogilvie, P. A. Bochsler, J. Geiss, "Ion composition experiment," Trans. Geosci. Electron., IEEE Trans. Geosci. Electron., GE-16, 185, 1978.

Eberhardt, P., J. Geiss, and N. Gröhler, "Ueber die Verteilung der Uredelgase im Meteoriten Khor Temiki," Tschermaks mineralogische und petrographische Mitteilungen, 10, 535-551, 1965a.

Eberhardt, P., J. Geiss, Grögler, "Further evidence on the origin of trapped gases in the meteorite Khor Temiki," J. Geophys. Res. 70, 4375-4378, 1965b.

Eberhardt, P., J. Geiss, H. Graf, N. Grögler, M. D. Mendi, M. Morgeli, H Schwaller, and A. Stettler, "Trapped solar wind noble gases in Apollo 12 lunar fines 12001 and Apollo 11 breccia 10046," Proc. 3rd Lunar Sci. Conf., Houston, Vol. 2, 1921-1956, 1972. Pergamon Press.

Fisk, L., "^{3}He-rich solar fluxes--a possible explanation," Ap. J. 224. 1048, 1978.

Garrard, T. L., E. C. Stone and R. E. Vogt in High Energy on the Sun Symposium Proceedings, R. Ramty and R. G. Stone, eds., NASA, SP 342, 1973, pp. 341.

Geiss, J., F. Bühler, H. Cerutte, P. Eberhardt and C. Filleaux, "Solar wind composition experiment," Apollo 16 Prel. Sci. Rep., pp. 14.1-14.10, NASA, SP-315, 1972.

Geiss, J., "Processes affecting abundances in the solar wind," Space Science Reviews, 33, 201, 1982.

Geiss, J., P. Hirt and H. Leutwyler, "On acceleration and ions in corona and solar wind," Solar Phys., 12, 458, 1970.

Geiss, J., "Solar wind composition and implications about the history of the Solar System" Proc. 14th Int. Cosmic Ray Conf. Denver, 5, 3375, 1973.

Geiss, J. and P. Bochsler, "On the abundances of rare ions in the solar wind," Pro. 4th Solar Wind Conf., Burghausen, Max-Planck-Institut für Aeronomie, Lindau, FRG, 1982.

Gosling, J. T., G. Borrini, J. R. Asbridge, S. J. Bame, W. C. Feldman, R. T.

Hansen, "Coronal streamers in the solar wind at 1 AU," J. Geophys, Res., 86, 5483, 1981.

Gumbel, E. J., Statistics of Extremes, Columbia University Press, N. Y., 1958, Chapter 1.

Grünwaldt, H., "Solar wind composition from the Heos-2 plasma experiment," Space Research, 16, 681, Academie-Verlag, Berlin, 1976.

Hall, D. N. B., Spectroscopic detection of solar ^{3}He," Astrophys. J., 197, 509-512, 1975.

Hintenberger, H., E. Vilcsek, and H. Wänke, Über Isotopenzusammensetzung und über den Sitz der Leichten Uredelgase in Steinmeteoriten," Z. Naturforschg. 20a. 939-945, 1965.

Hirshberg, J., A. Alksne, D. S. Colburn, S. J. Bame, A. J. Hundhausen, "Observations of a solar flux induced interplanetary shock and helium-enriched driver gas," J. Geophys. Res., 75, 1, 1970.

Hollweg, J., "Minor ions in the low corona," J. Geophys. Res., 87, 8899, 1981.

Howard, R. A. and M. J. Roomen, "Observation of sectored structure in the outer solar corona; correlation with interplanetary magnetic field," Solar Phys. 37, 469, 1974.

Hsieh, K. C. and J. A. Simpson, "The relative abundances and energy spectra of ^{3}He and ^{4}He from solar flares," Astrophys. J., 162, L191-L196, 1970.

Kunz, S., P. Bochsler, J. Geiss, M. A. Coplan, K. W. Ogilvie, "Determination of solar wind elemental abundances from M/Q observations during three periods in 1980," Solar Physics, in press, 1983.

Neugebauer, M. and C. W. Snyder, "Mariner 2 observations of the solar wind," J. Geophys. Res., 71, 4469, 1966.

Neugebauer, M., "Observations of solar wind helim," Solar wind four, M. Neugebauer ed., Report No. MPAE-W-100-81-31, p. 425, 1981.

Ogilvie, K. W. and L. F. Burlaga, "A discussion of interplanetary post-shock flows with two examples," J. Geophys. Res. 79, 2324 (1974).

Ogilvie, K. W., M. A. Coplan, P. Bochsler, J. Geiss, "Abundance ratios of $^4He^{++}$ in the solar wind," J. Geophys Res., 85, 6021, 1980a.

Ogilvie, K. W., P. Bochsler, J. Geiss, M. A. Coplan, "Observations of the velocity distribution of solar wind ions," J. Geophys. Res., 85, 6069, 1980b.

Pneuman, G. W. and R. A. Kop, "Coronal Streamers, II," Solar Physics, 13, 176, 1970.

Reames, D. V. and T. von Rosenvinge, "Heavy element abundances in helium 3-rich events, Proc. 17th Int. Cosmic Ray Conf., 3, 162, 1981.

Rosenbauer, H., R. Schwenn, E. Marsch, B. Meyer, H. Biggenrieder, M. D. Montgomery, K. H. Mühlauser, W. Pilipp, W. Voges and S. M. Znik, "A survey on initial results of the Helios plasma experiment," Journal of Geophysics, 421, 561, 1977.

Schatzman, E. and A. Maeder, "Stellar evolution with turbulent diffusion mixing III. The solar model and the neutrino problem," Astron. Astrophys. 96, 1-16, 1981.

Schmidt, W. K. H., H. Rosenbauer, E. G. Shelly, and J. Geiss, "On temperature and speed of He^{++} and O^{6+} ions in the solar wind, "Geophys. Res. Lett. 7, 697-700, 1980.

Wänke, H., "Der Sonnenwind als Quelle der Uredelgase in Steinmeteoriten," Z. Naturforschg, 20a, 946-949, 1965.

Warasil, R. L. and A. Schaeffer, "Trapped solar wind He, Ne, and Ar and energetic He in Surveyor 3," Earth Planet. Sci. Lett., 24, 71-77, 1974.

Zähringer, J., "Über die Uredelgase in den Chondriten Kapoeta und staroe Pesijaneo," Geochim. Cosmochim. Acta, 26, 665-680, 1962.

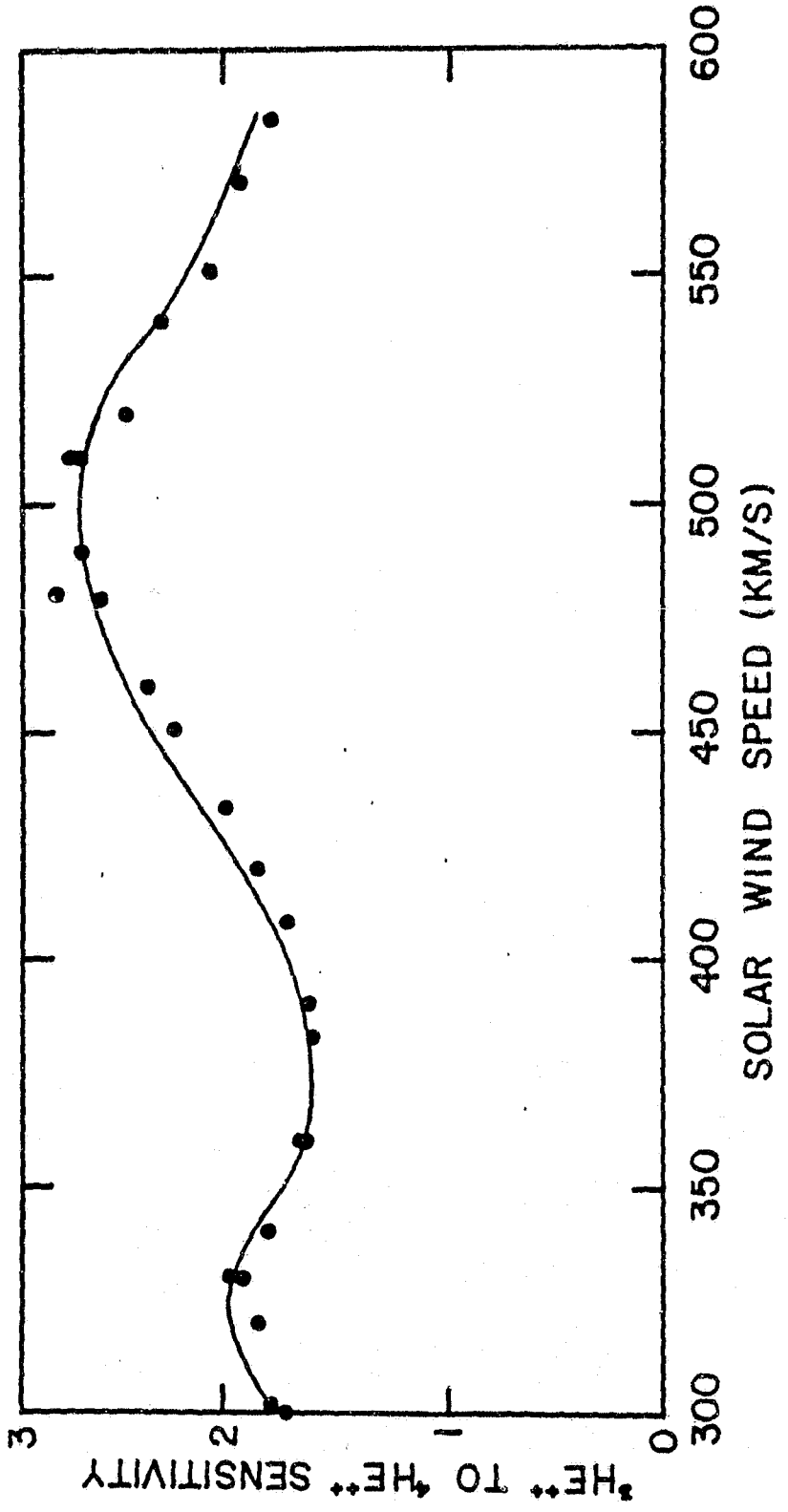

Figure 1

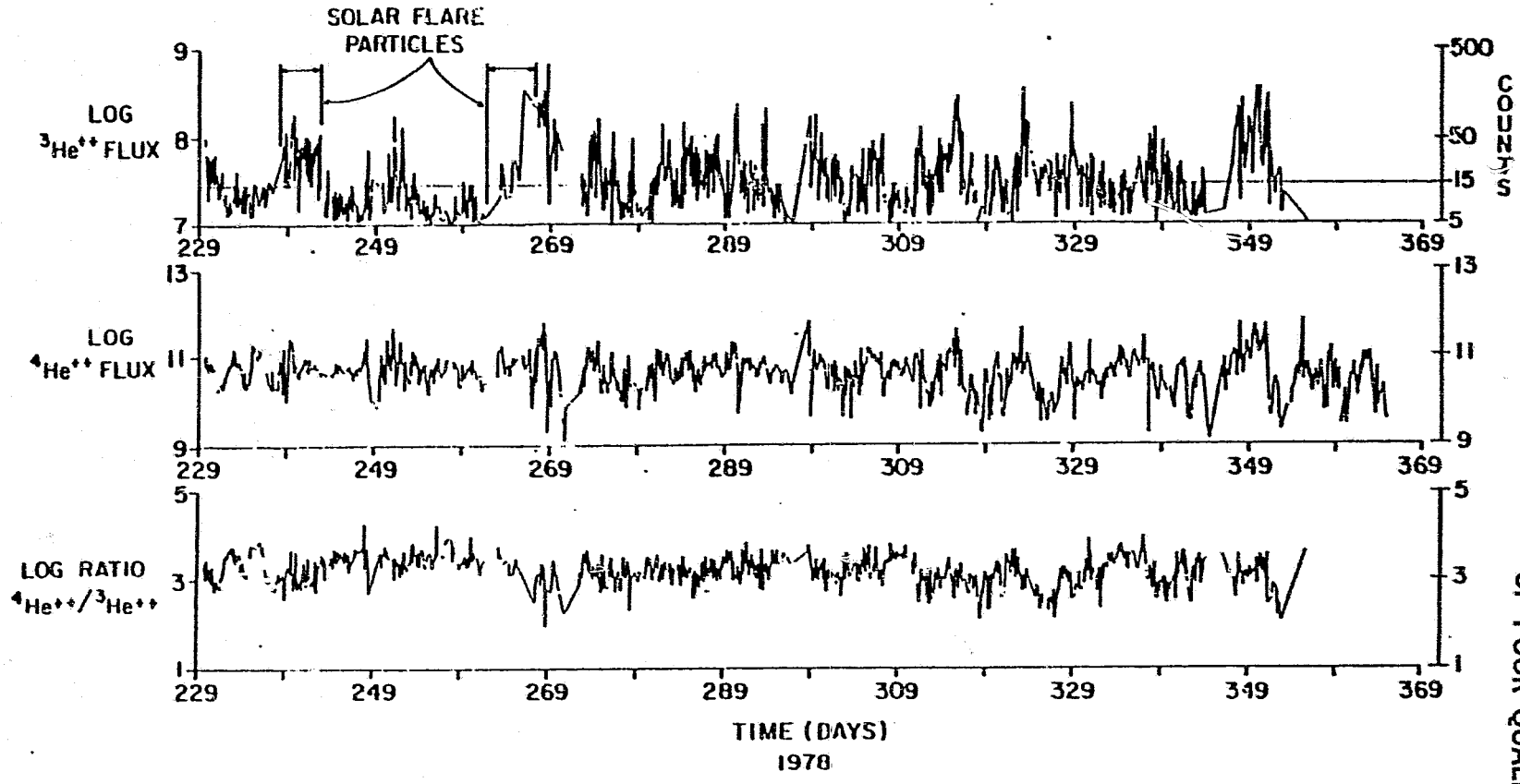

Figure 2

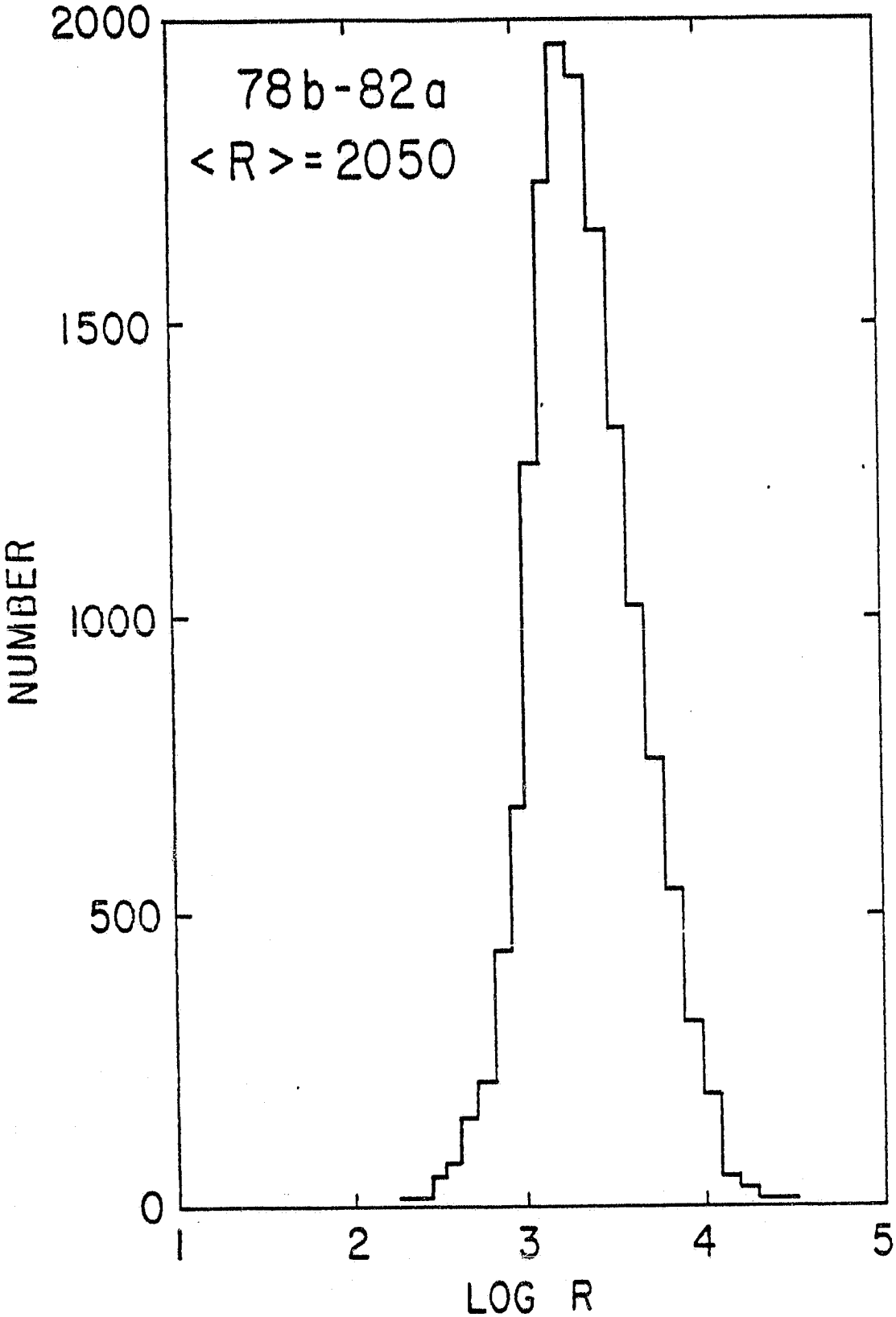

Figure 3a

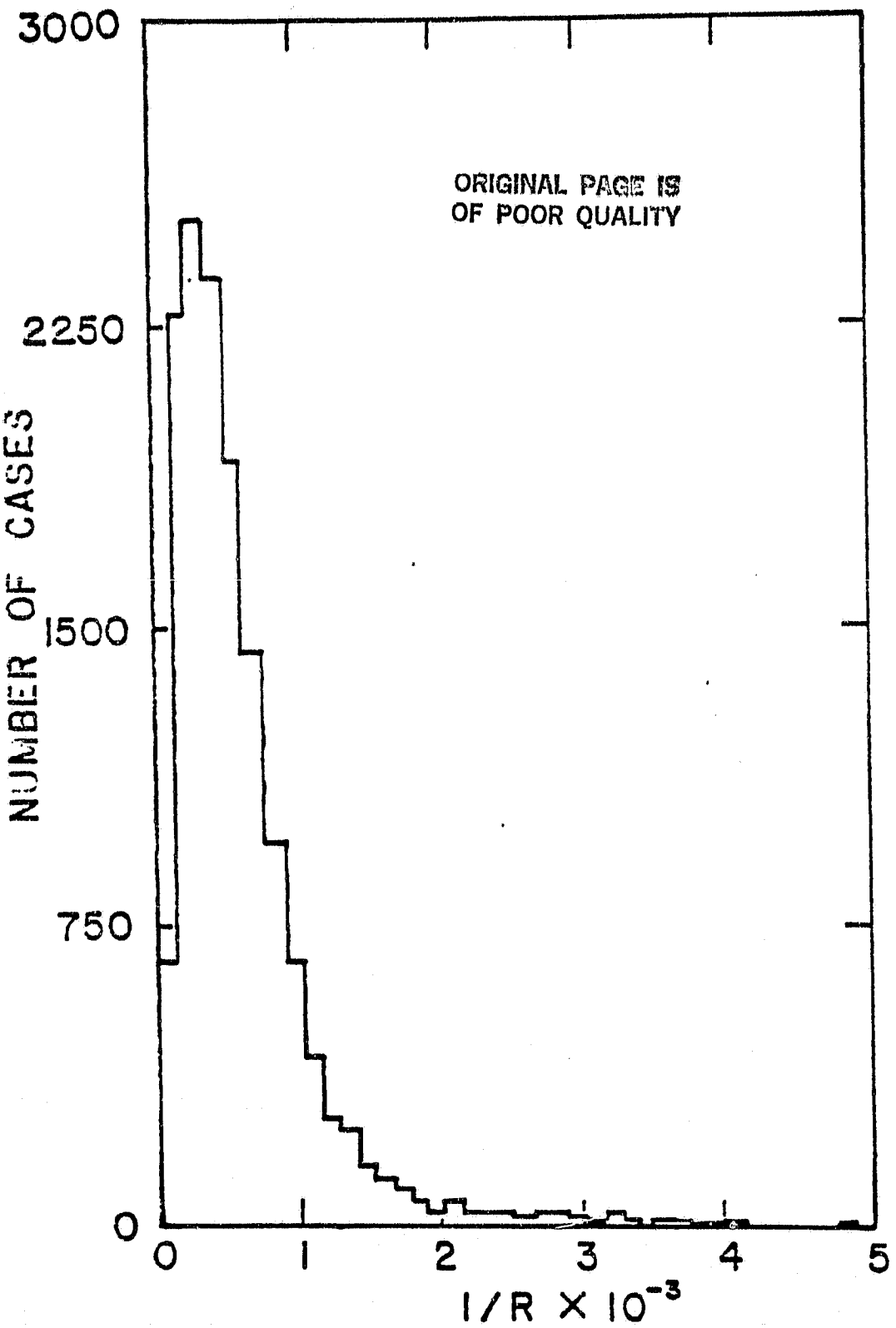
3000
2250
1500
750
0
NUMBER OF CASES
0
1
2
3
4
5
1/R X 10⁻³
ORIGINAL PAGE IS
OF POOR QUALITY

Figure 3b

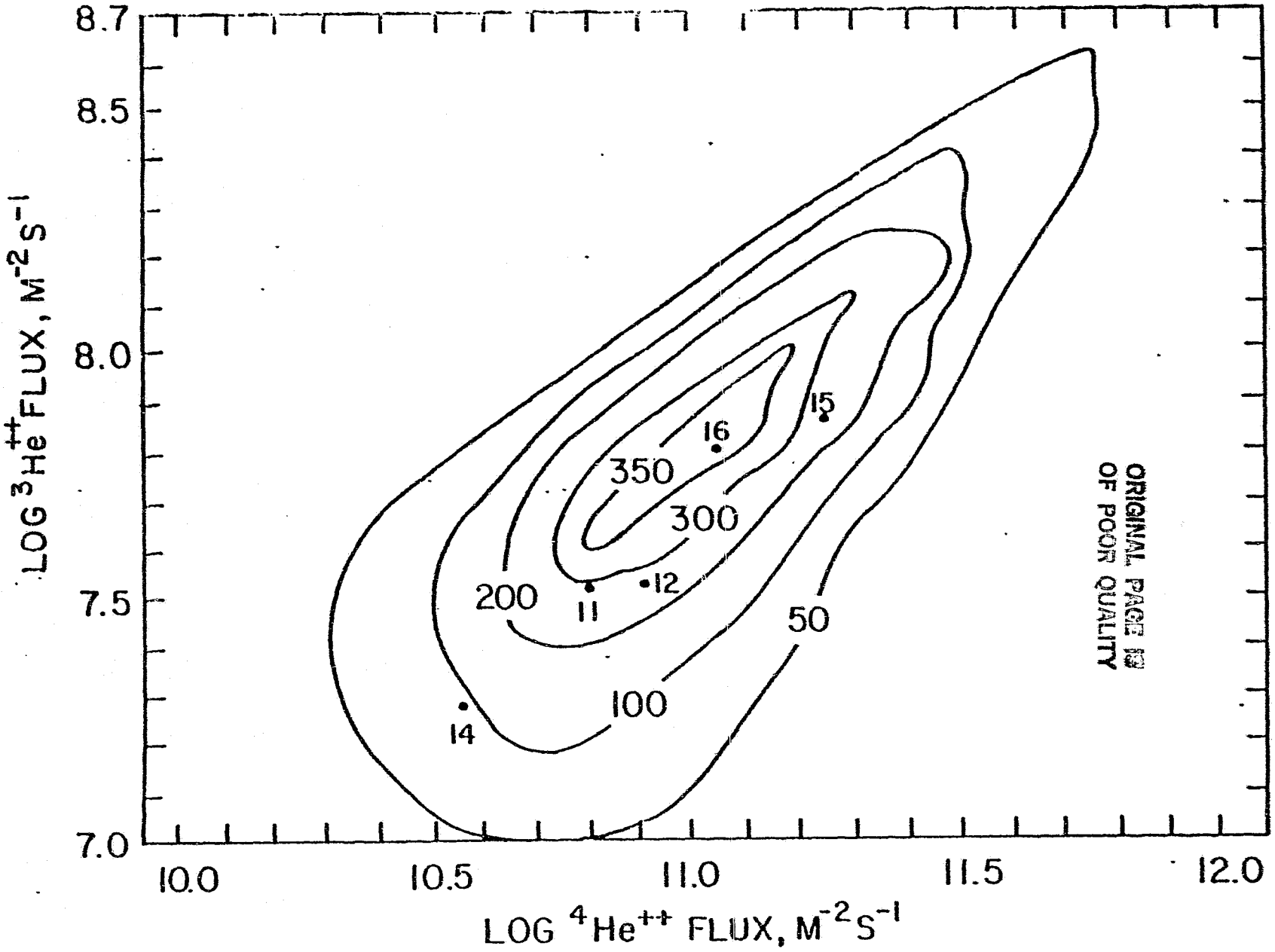
8.7
8.5
8.0
7.5
7.0
LOG $^{3}He^{++}$ FLUX, $M^{-2}S^{-1}$
10.0
10.5
11.0
11.5
12.0
LOG $^{4}He^{++}$ FLUX, $M^{-2}S^{-1}$
350
300
200
100
50
11
12
14
15
16
ORIGINAL PAGE IS
OF POOR QUALITY

Figure 4

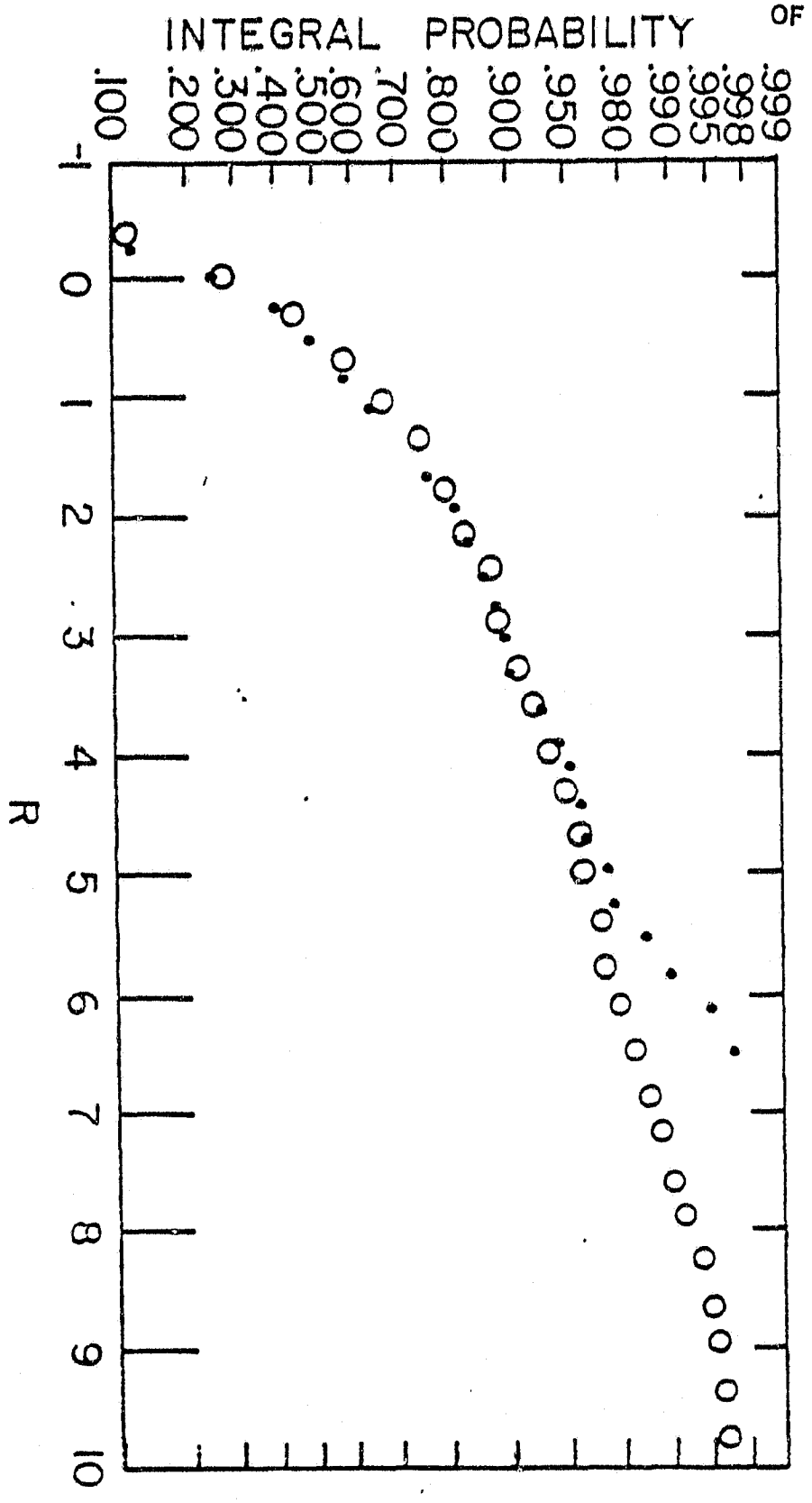

Figure 5

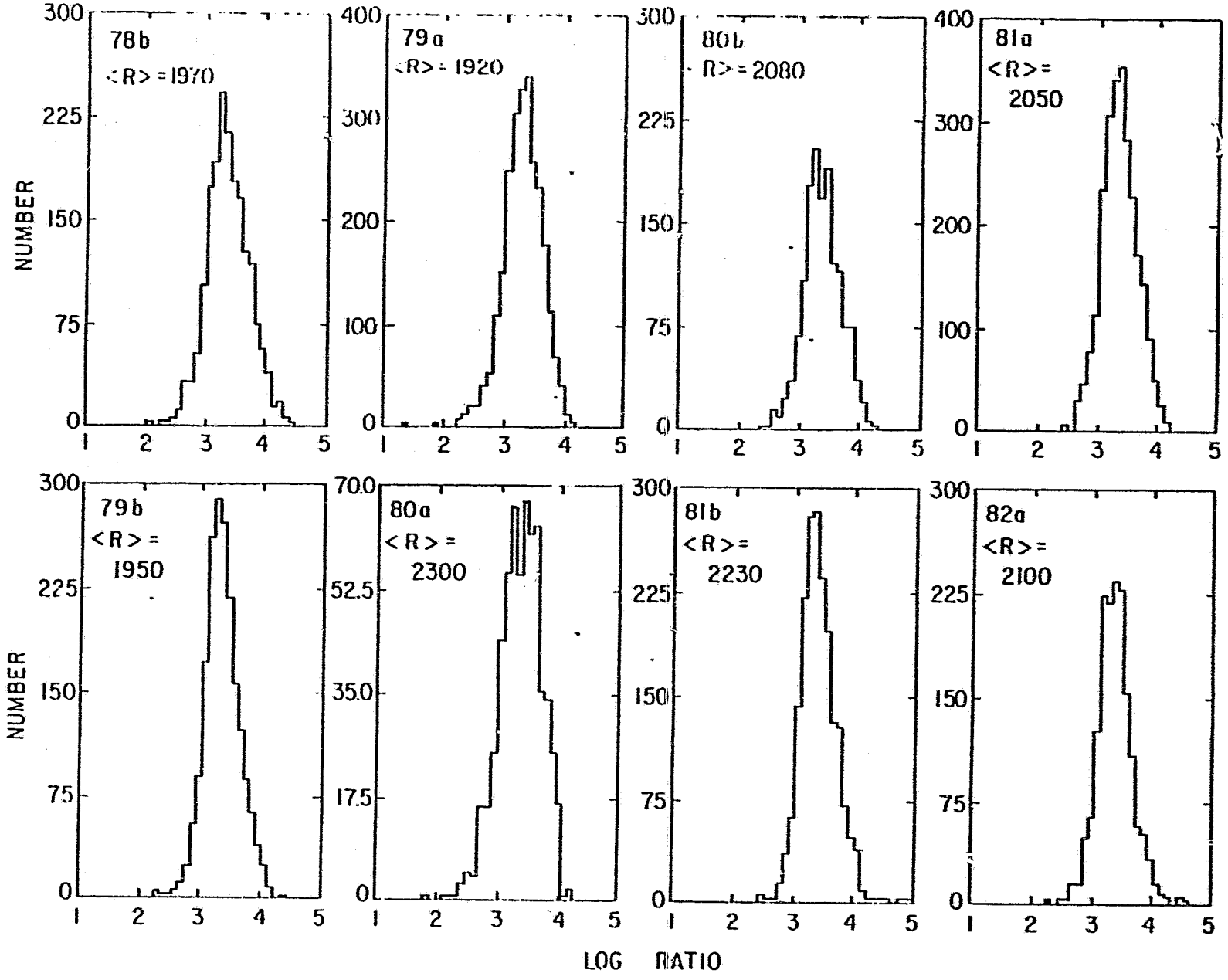

Figure 6

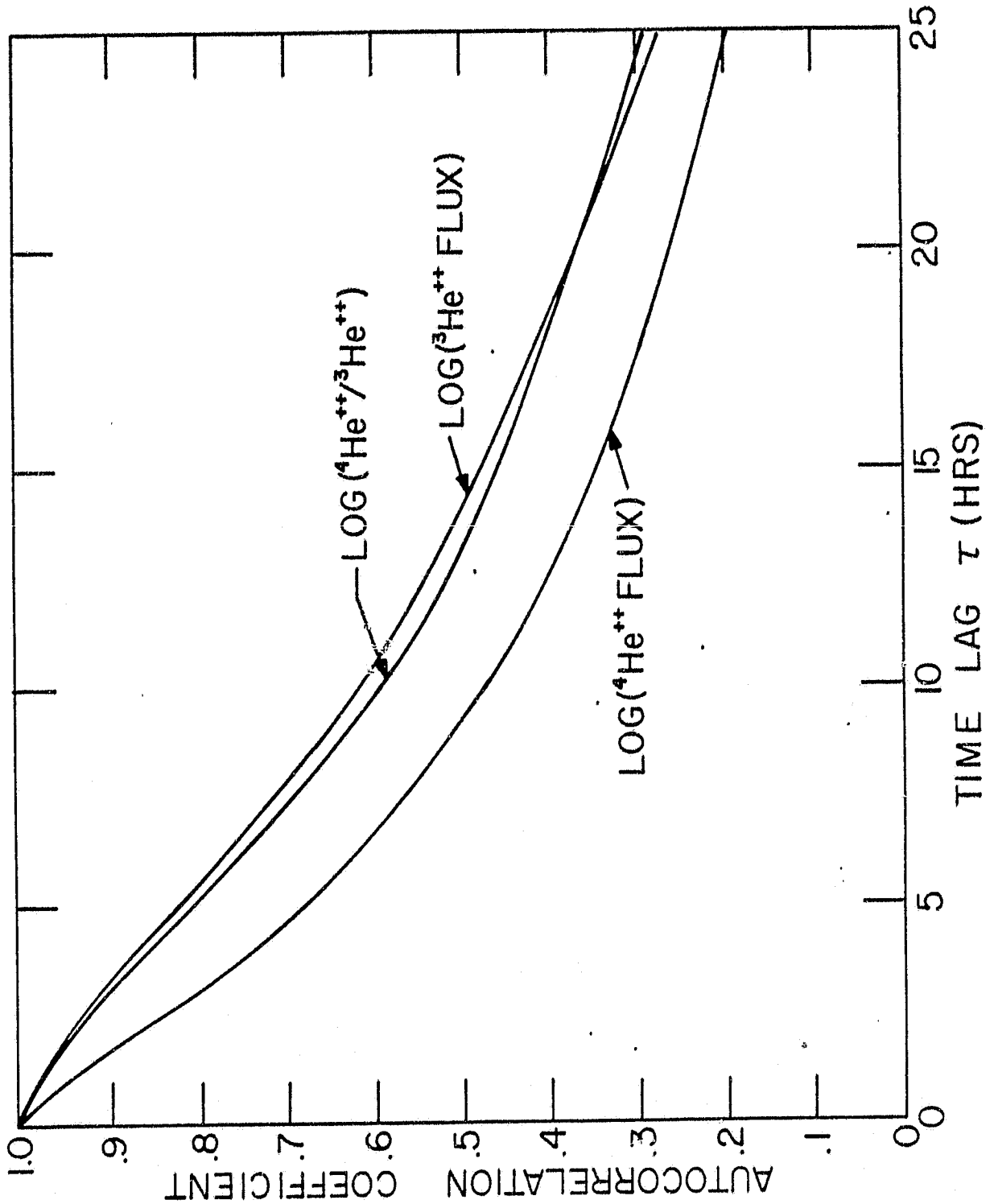

Figure 7

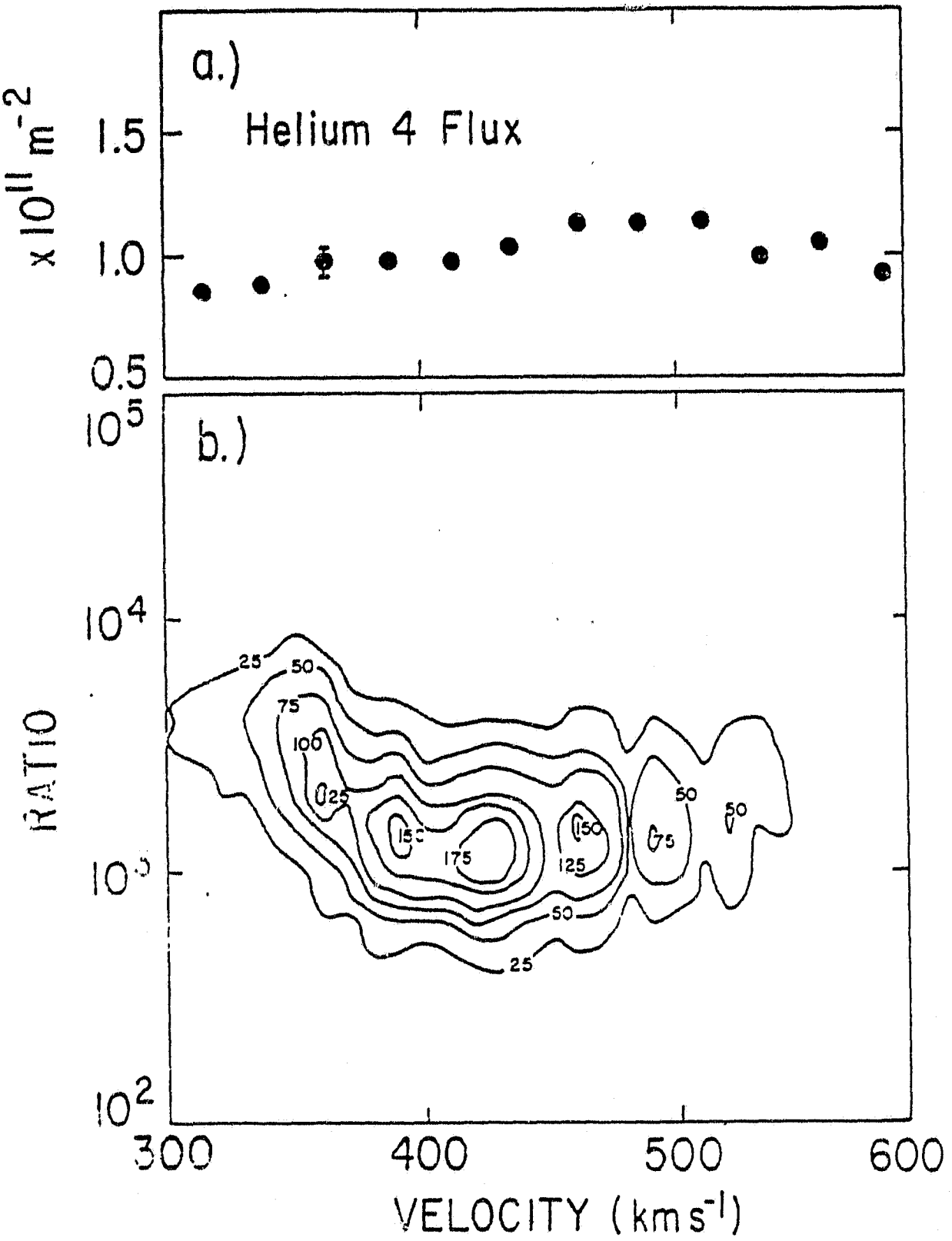

Figure 8

Fig 9

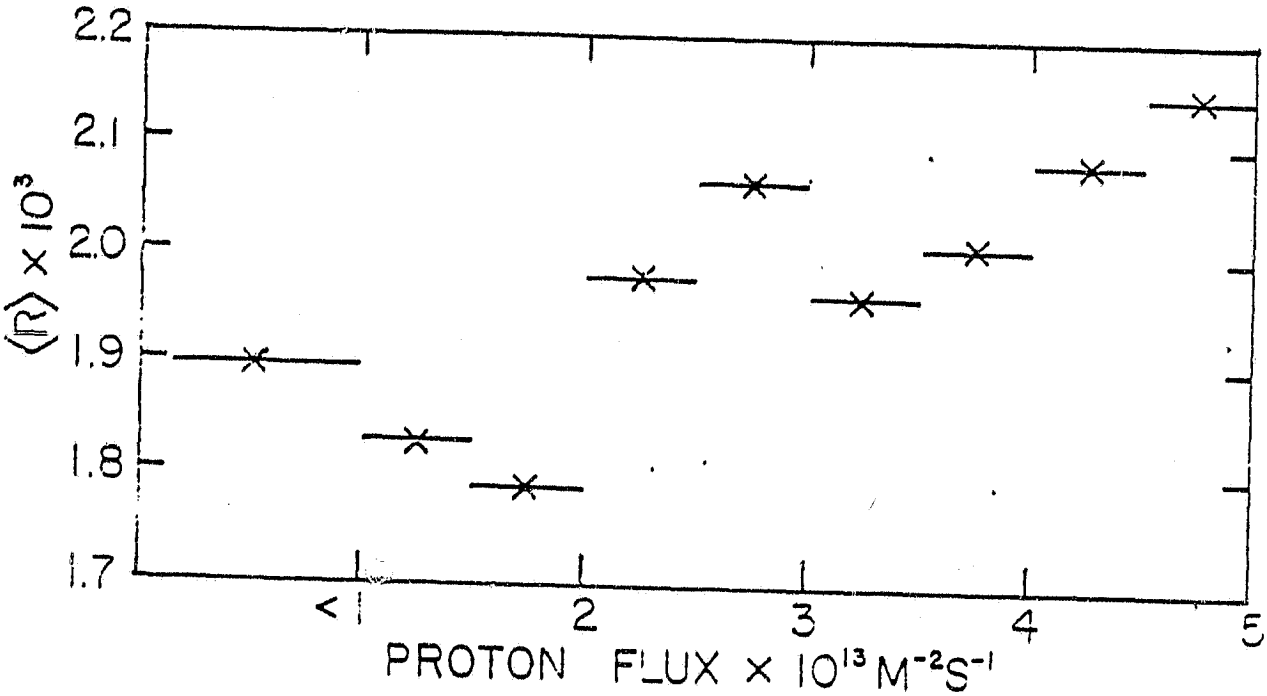

Figure 9

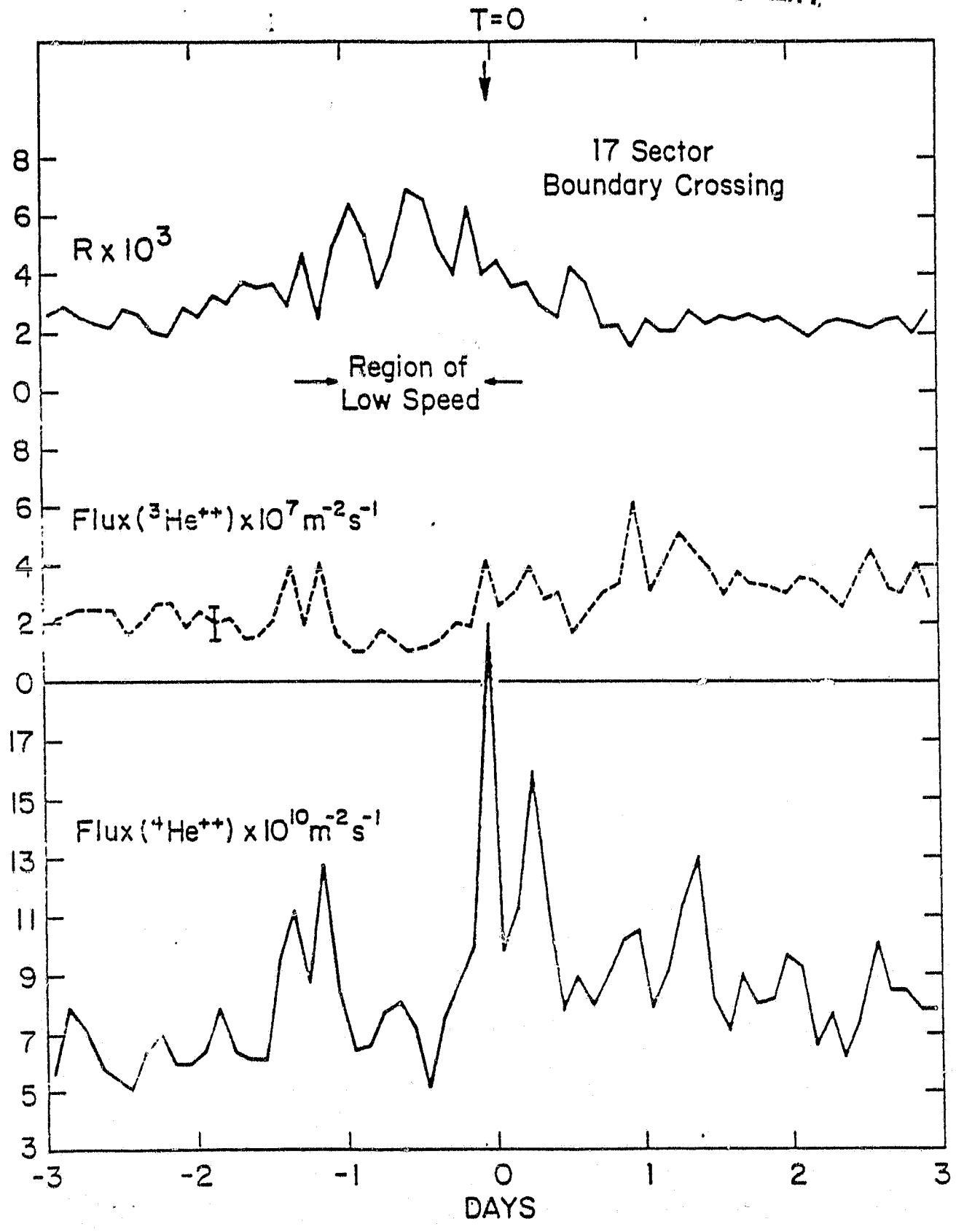

Figure 10

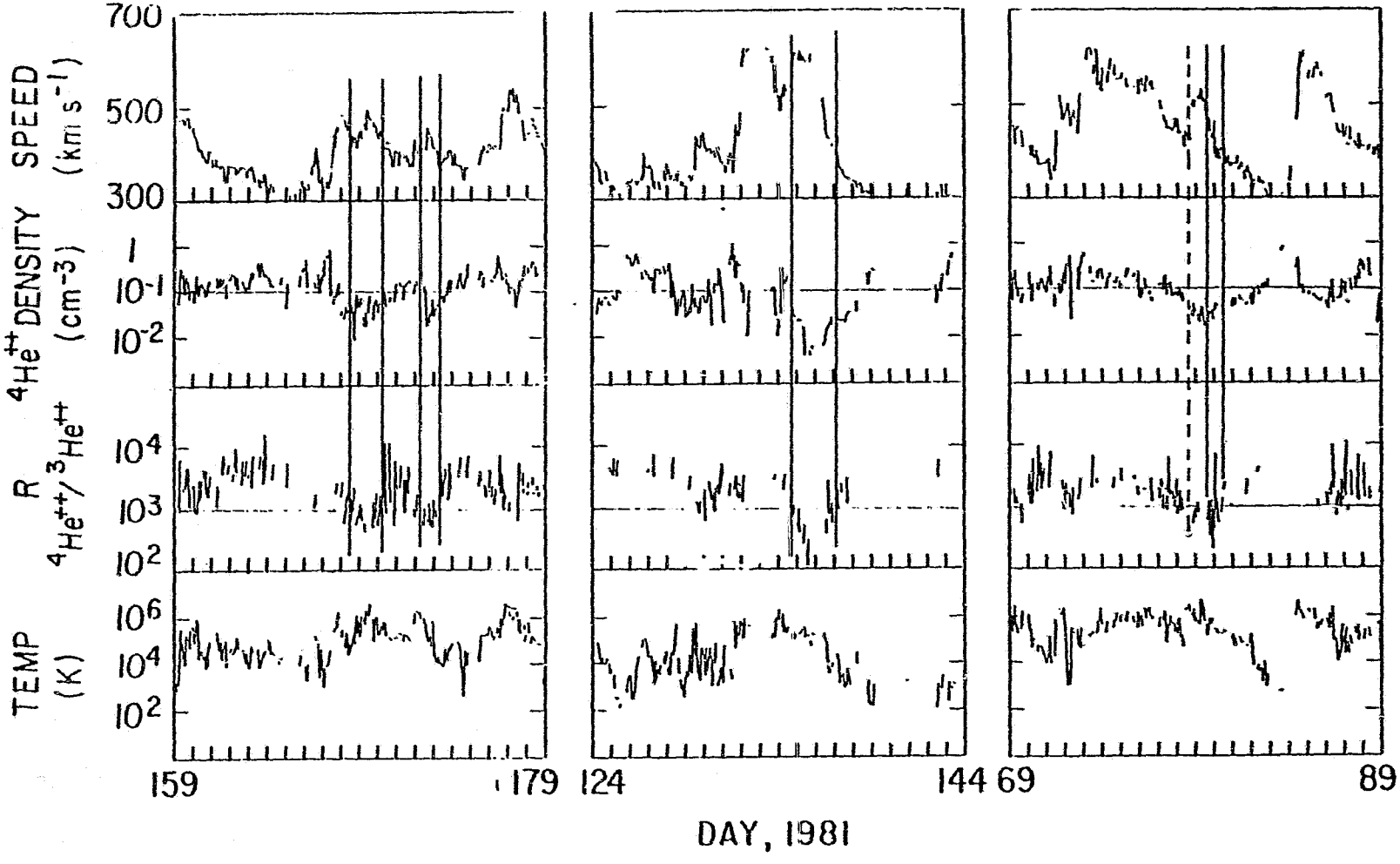

ORIGINAL PAGE IS
OF POOR QUALITY

Figure 11

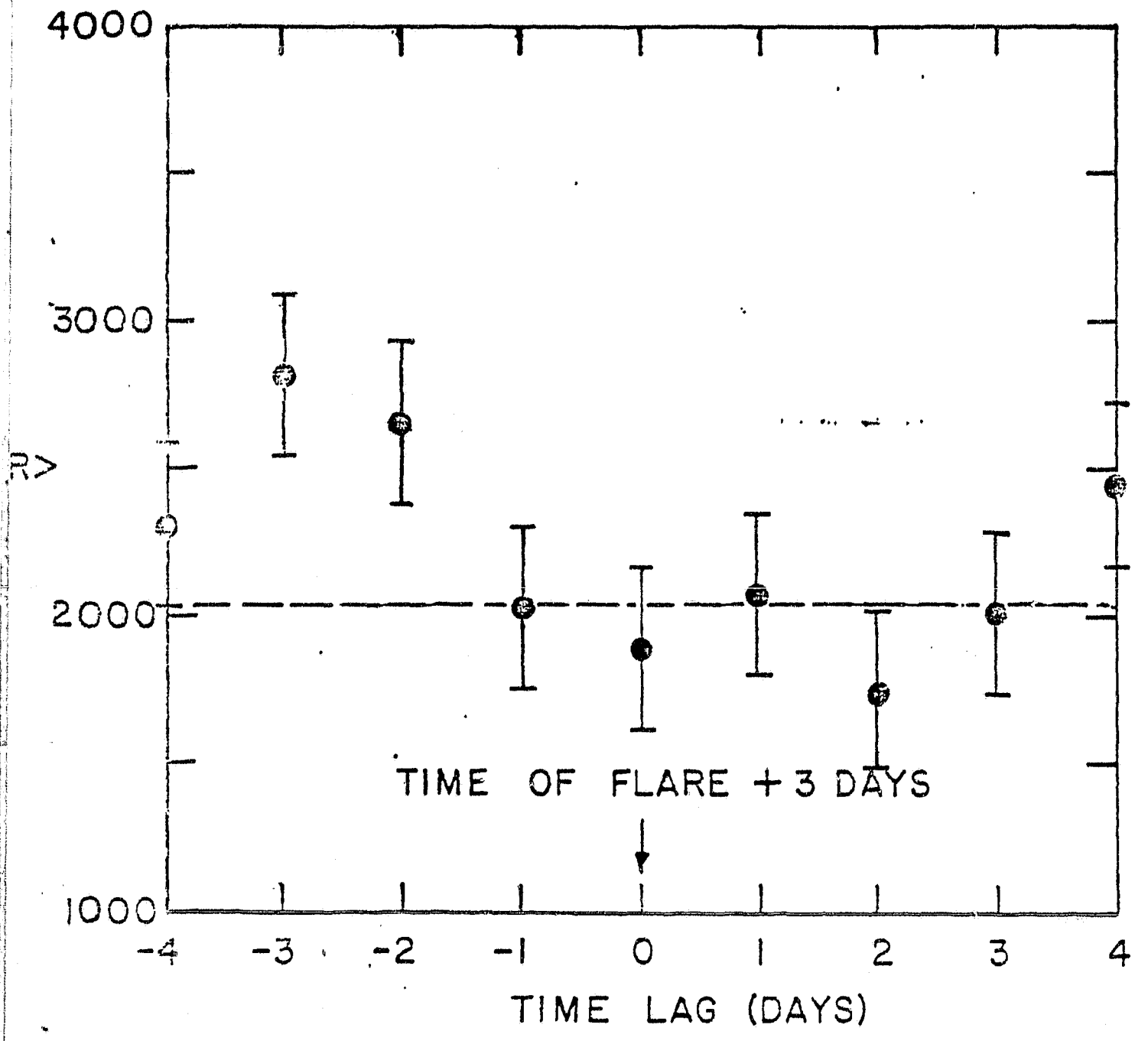

Figure 12